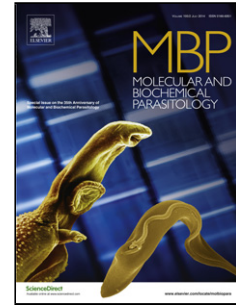


Accepted Manuscript

Title: Screening of the MMV and GSK open access chemical boxes using a viability assay developed against the kinetoplastid *Crithidia fasciculata*

Authors: Wakisa Kipandula, Simon A. Young, Stuart A. MacNeill, Terry K. Smith



PII: S0166-6851(18)30101-4
DOI: <https://doi.org/10.1016/j.molbiopara.2018.05.001>
Reference: MOLBIO 11126

To appear in: *Molecular & Biochemical Parasitology*

Received date: 1-12-2017
Revised date: 19-4-2018
Accepted date: 1-5-2018

Please cite this article as: Kipandula W, Young SA, MacNeill SA, Smith TK, Screening of the MMV and GSK open access chemical boxes using a viability assay developed against the kinetoplastid *Crithidia fasciculata*, *Molecular and Biochemical Parasitology* (2018), <https://doi.org/10.1016/j.molbiopara.2018.05.001>

This is a PDF file of an unedited manuscript that has been accepted for publication. As a service to our customers we are providing this early version of the manuscript. The manuscript will undergo copyediting, typesetting, and review of the resulting proof before it is published in its final form. Please note that during the production process errors may be discovered which could affect the content, and all legal disclaimers that apply to the journal pertain.

Short communication

**Screening of the MMV and GSK open access chemical boxes using a viability assay
developed against the kinetoplastid *Crithidia fasciculata***

Wakisa Kipandula^{a,b}, Simon A. Young^a, Stuart A. MacNeill^a and Terry K. Smith^{a*}

^a Biomedical Sciences Research Complex, University of St Andrews, North Haugh, St Andrews, Fife KY16 9ST, UK.

^b Department of Medical Laboratory Sciences, College of Medicine, University of Malawi, Private Bag 360, Chichiri, Blantyre 3, Malawi.

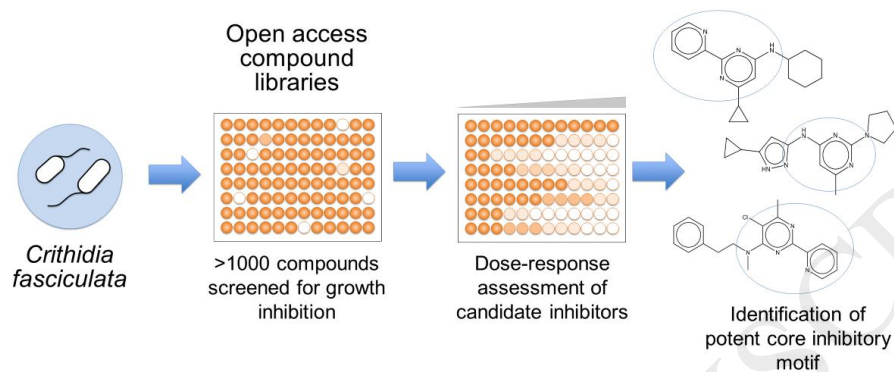
* Corresponding author

Email: tksl@st-and.ac.uk

Tel. (+44) 1334 463412

Graphical abstract

Screening open access compound libraries to identify novel inhibitors of the growth of the kinetoplastid parasite *Crithidia fasciculata*



Highlights (3-5 bullet points, 85 characters max. per bullet point)

- *C. fasciculata* is a low-cost non-human infectious model for kinetoplastid biology
- >1000 compounds from open access libraries screened for *C. fasciculata* inhibition
- Dose-response testing confirmed inhibitory activity
- Several inhibitors share a 2-(pyridin-2-yl) pyrimidin-4-amine scaffold

Abstract

Diseases caused by the pathogenic kinetoplastids continue to incapacitate and kill hundreds of thousands of people annually throughout the tropics and sub-tropics. Unfortunately, in the countries where these neglected diseases occur, financial obstacles to drug discovery and technical limitations associated with biochemical studies impede the development of new, safe, easy to administer and effective drugs. Here we report the development and optimisation of a *Crithidia fasciculata* resazurin viability assay, which is subsequently used for screening and identification of anti-crithidial compounds in the MMV and GSK open access chemical boxes. The screening assay had an average Z' factor of 0.7 and tolerated a maximum dimethyl sulfoxide concentration of up to 0.5%. We identified from multiple chemical boxes two compound series exhibiting nanomolar potency against *C. fasciculata*, one centred around a 5-

nitrofurantoin scaffold, a well-known moiety in several existing anti-infectives, and another involving a 2-(pyridin-2-yl) pyrimidin-4-amine scaffold which seems to have pan-kinetoplastid activity. This work facilitates the future use of *C. fasciculata* as a non-pathogenic and inexpensive biological resource to identify mode of action/protein target(s) of potentially pan-trypanocidal potent compounds. This knowledge will aid in the development of new treatments for African sleeping sickness, Chagas disease and leishmaniasis.

Keywords : *Crithidia fasciculata*, *kinetoplastid*, *drug discovery*

Introduction

The trypanosomatidae family comprises several genera, some of which undergo cyclical development in both vertebrate and invertebrate hosts. These include the mammalian infective *Trypanosoma* and *Leishmania* species, responsible for potentially fatal diseases in both humans and animals. About half a billion people dwelling in tropical and sub-tropical areas of the World are at risk of contracting these diseases, with more than 20 million people infected with the pathogens that cause them, resulting in extensive suffering and more than 100,000 deaths per year [1].

The treatment options for the neglected tropical diseases caused by these pathogens have always been limited to a few relatively ineffective drugs, most of which were discovered over 50 years ago. These drugs have been reported to possess several drawbacks and limitations in their efficacy. For example, the conventional drugs for treating Human African Trypanosomiasis (HAT) such as Suramin, Pentamidine, Melarsoprol and Eflornithine vary in effectiveness depending on the stage of the disease and the trypanosome species involved, require long periods of administration and are associated with toxicities and drug resistance [2]. Chagas disease front-line drugs Nifurtimox and Benznidazole are associated with severe side effects, long treatment periods (>60 days) and variations in sensitivity of the parasites [3-4]. Miltefosine is currently the only oral treatment for visceral leishmaniasis (VL), but its clinical use has been limited due to its teratogenic effects and increasing reports of treatment failures [5]. AmBisome, previously considered effective against VL, requires intravenous administration, is very expensive and is associated with side effects. The lack of formulations for paediatric patients and pregnant women and the unavailability of these trypanosomatid drugs due to low production [6] are clear obstacles in terms of drug accessibility to the people who really need them. There is, therefore, an urgent demand to identify novel drug targets and develop new therapies for these neglected diseases.

One approach to drug discovery is through high throughput screening (HTS) of diverse compound collections for identification of active hits by whole cell screening. Although several efforts have been made, drug discovery through HTS for these trypanosomatid diseases has been a slow process. This has been due, among other reasons, to a requirement for expensive containment facilities and costly serum-containing media, essential for propagation of these parasites. These and other factors renders drug discovery through HTS for these parasites impractical in resource-limited countries where the burden of the disease is highest.

Crithidia fasciculata is a non-mammalian infective lower trypanosomatid, which can be handled in a standard laboratory without specific biosafety issues. *C. fasciculata* has relatively fast growth kinetics and can be easily and inexpensively grown to high cell densities in liquid media, which can be fully defined and serum-free. *C. fasciculata* represents a very interesting model to study biological cellular and genetic processes unique to members of the family Trypanosomatidae. This kinetoplastid has a very similar cellular machinery and is phylogenetically related to the human pathogenic trypanosomatids (*T. brucei*, *T. cruzi* and especially *Leishmania spp.* with whom it is more closely related) and is easily amenable to molecular, genetic and biochemical analyses.

Over the past few decades *C. fasciculata* has been utilised as a model system to study the biochemical, cellular, and genetic processes unique to members of the family Trypanosomatidae. This has allowed researchers to uncover cellular and/or biochemical processes that ultimately could be exploited for the development of novel therapies for the related pathogenic trypanosomatids [7-12].

Although it should be noted that *C. fasciculata* are unable to invade / and are non-pathogenic to mammalian cells, and certain aspects of their proteome and mitochondria are different compared to *Leishmania*, probably reflecting differences in their carbon-source usage [13].

Here we explore the use of *C. fasciculata* as a low-cost model organism in determining the anti-crithidial activities of compounds from collections known to have anti-parasitic activity. We repurposed the current Medicines for Malaria venture (MMV) Pathogen box (<http://www.mmv.org/>) and the GlaxoSmithKline (GSK) Tres Cantos anti-kinetoplastid chemical boxes to screen for compounds active against *C. fasciculata*. The MMV chemical box contains 402 diverse drug-like compounds selected with activity against diseases such as Chagas disease, malaria, HAT, tuberculosis and schistosomiasis [14]. The GSK anti-kinetoplastid compounds are assembled into three boxes according to the organism they are

most active against i.e. *L. donovani* (Leish-Box), *T. cruzi* (Chagas-Box) and *T. brucei* (HAT-Box), with each box containing ~200 compounds [15]. These chemical boxes have been assembled and all data made publically available (<https://www.ebi.ac.uk/chemblntd>) with the aim of facilitating and stimulating the drug discovery for these neglected diseases.

Materials and methods

Reagents

All chemicals and reagents used in the experiments were purchased from Sigma-Aldrich.

Parasites and cell culture

The *C. fasciculata* promastigotes clone HS6 were grown at 27°C with gentle agitation in axenic serum-free defined media containing yeast extract (5 mg/mL), tryptone (4 mg/mL), sucrose (15 mg/mL), triethanolamine (4.4 mg/mL) and Tween 80 (0.5%) and supplemented with 10 µg/mL of haemin. The parasites were sub-cultured every 2-3 days to ensure log growth phase for subsequent experiments.

Compound libraries

Chemical boxes were kindly provided by MMV and GSK Tres Cantos. The MMV pathogen box contained 402 chemicals representing compounds that were active against one or more of 12 distinct pathogens (see <https://www.pathogenbox.org/about-pathogen-box/supporting-information>). Individual compounds had only been tested to confirm activity against the pathogen for which the compounds were first reported to be active, and have not been tested against the other pathogens represented in the pathogen box. All compounds have been tested for cytotoxicity: typically, they were five-fold less potent against a human fibroblast cell line (MRC-5) than the pathogen (<https://www.pathogenbox.org/about-pathogen-box/supporting-information>).

The three GSK kineto boxes (Leish-Box, Chagas-Box and HAT-Box), with each box containing ~200 compounds assembled by Pena and his colleagues [15] as previously discussed, were donated by GSK Tres Cantos. The supplied information included details on the pathogen against which the compound had shown activity, compound cytotoxicity, as well as other useful data such compound ID, batch ID, trivial name, molecular weight, salt, and cLogP. More information about these compounds can be accessed online via ChEMBL-NTD (<https://www.ebi.ac.uk/chemblntd>).

Both the MMV and the GSK compounds were supplied in 96-well plates, containing 10 µL of 10 mM dimethyl sulfoxide (DMSO) solution of each compound. Each compound was then diluted with phosphate buffer saline (PBS) to a working concentration of 2.5 mM (DMSO,

25%) and aliquoted into multiple plates. The compounds were stored at -80°C and thawed at room temperature prior to use. Each of the 400 compounds was screened in quadruplicate at a concentration of $100\ \mu\text{M}$ (DMSO, 0.5% final concentration) in 96-well plates.

***C. fasciculata* viability assay optimization**

Although resazurin-reduction assay has been extensively used for screening drug susceptibility of various cell types, it has not yet been applied to *Crithidia*. Therefore, a number of conditions such as the growth kinetics of cells, maximum cell densities, the incubation period, the resazurin concentration and the DMSO concentrations had to be considered and optimised for the resazurin-reduction assay to work as a screening tool in this system. A stock solution of $12.5\ \text{mg/mL}$ resazurin in PBS was used in all assays. All fluorescence measurements in this study were performed with the Spectra Max Gemini XPS Microplate reader (Molecular Devices) with excitation and emission wavelengths of $560\ \text{nm}$ and $590\ \text{nm}$.

Multiplicative kinetics of *C. fasciculata*

Cell densities of three replicate cultures starting at 1×10^3 , 1×10^4 and 3×10^4 cells/mL were microscopically monitored and counted using a haemocytometer at 24 hour intervals, over 5 days. A growth curve was plotted to estimate the maximum number of cells attainable in a 96-well plate before stationary phase and possible cell death occur.

Effect of time and volume on resazurin fluorescence development

In order to determine the fluorescent development at different volumes of the dye and the incubation period, *C. fasciculata* choanomastigotes (5×10^4 cells/mL) were incubated in the presence of various resazurin volumes (5, 10, 15 or $20\ \mu\text{L}$ of a $12.5\ \text{mg/mL}$ stock) and monitored after every 1 hour for a period of 4 hours. After 4 hours of incubation, the fluorescent signal became saturated and the less dye in the medium, the more rapidly it was completely reduced by the cells and became colourless and non-fluorescent. The experiments were performed twice and the results were averaged over eight replicate wells.

Determining the relationship between cell density and the resazurin fluorescence

To determine the relationship between cell density and the fluorescence signal, the parasites in the logarithmic phase of a stock suspension of 1×10^6 cells/ml were serially diluted ($100\ \mu\text{L}$) into 96-well plates followed by addition of $10\ \mu\text{L}$ of resazurin. Plates were incubated at 27°C and fluorescence measured after every 1 hour for a period of 4 hours. The experiments were performed twice and the results were averaged over eight replicate wells.

Determining the effect of DMSO concentrations on the assay signal

$90\ \mu\text{L}$ of medium containing *C. fasciculata* choanomastigotes ($5,000$ cells/mL) was inoculated into a 96-well plate and incubated for 24 hours. $10\ \mu\text{L}$ of various (0.5 – 9.0 % final)

concentrations of DMSO diluted in the medium were then added to the plates and further incubated for 24 hours. The experiments were performed twice and the results were averaged over eight replicate wells.

Primary screening assays

C. fasciculata choanomastigotes in the log phase of growth were diluted 1:20 in the axenic growth media, and 20 μL was counted using a hemocytometer. For anti-critidial activity, compounds were added to the test plates with medium containing the parasites (density $\sim 5 \times 10^4$ cells/ml) to achieve a final compound and DMSO concentration of 100 μM and 0.5%, respectively. The controls on each plate included wells containing growth media with 0.5% DMSO without cells (positive control) and growth media with 0.5% DMSO with cells only (negative control). The activities of test compounds were normalized against controls from the same plate according to the following formula: activity (%) = $[1 - (F_{\text{Cpd}} - F_{\text{Pos}}) / (F_{\text{Neg}} - F_{\text{Pos}})] \times 100$, where F_{Cpd} corresponds to the emitted fluorescent signal expressed in arbitrary fluorescence units for the test compound, and F_{Neg} and F_{Pos} correspond to the mean fluorescent signal of the negative and the positive control wells, respectively. For estimation of the hit confirmation rate, compounds were considered confirmed when the normalized anti-parasitic activity was equal to or greater than 80% ($\geq 80\%$) at 100 μM concentration.

Dose-response assessments of active compounds

The compounds which showed $\geq 80\%$ inhibition when tested at 100 μM concentration in at least one biological replicate were retested in 10-point dose response, two-fold serial dilution experiments starting at various compound concentrations with the parasites seeding density of $\sim 5 \times 10^4$ cells/mL. Wells containing the 0.5% DMSO growth media with no cells and 0.5% DMSO growth media with cells but no drug, served as 100% inhibition and 100% growth controls, respectively. 10 μL of the resazurin solution was added after 44 hours incubation and fluorescence development was determined after a total drug exposure time of 48 hours. The obtained fluorescence data was analysed with the graphic data analysis software GraFit (Erithacus Software) which calculated EC_{50} values by linear regression from the sigmoidal dose inhibition curves. Compounds which did and did not yield an EC_{50} value within the confines of the analysis parameters were simply expressed as the *true active* and *false active* compounds, respectively. A few compounds of interest, which had comparably low EC_{50} values were selected from the top ten lists, purchased from commercial sources (Sigma-Aldrich) and screened to finally confirm their activities. EC_{50} was defined as the concentration of a compound required to decrease the *C. fasciculata* viability by 50% compared to those grown

in the absence of the test compound. All experiments were performed twice, with each drug concentration in quadruplicate. For standardisation, EC_{50} values were converted to pIC_{50} .

Results and discussion

Resazurin-reduction *C. fasciculata* cell-based assay optimization

In order to determine the maximum cell numbers that could be used for developing the screening assay, the growth kinetics of *C. fasciculata* parasites growing in our formulated serum-free medium was analysed using the growth curve shown in **Supplementary Figure 1**. The parasites grew quite robustly under axenic conditions *in vitro* and reached the stationary phase after 3 days. Similar *C. fasciculata* growth kinetics for *in vitro* culture systems have been reported elsewhere [16-17]. The average generation time was determined according to the Popp and Lattorff [18] equation and gave an estimation of approximately 4.5 hours. The doubling time observed is shorter than the doubling time (6.8 hours) reported for *T. brucei brucei* bloodstream forms when grown in HMI-9 supplemented with 10% foetal calf serum [18] and 7 hours for some *Leishmania* species (S. Menzies, personal communication).

A linear relationship was observed between the incubation time and the fluorescent development of resazurin reduction (**Supplementary Figure 2**). However, low dye concentrations gave relatively higher fluorescent signal as compared to higher concentrations. A similar independent relationship between resazurin concentration and the fluorescent signal have been previously reported in alternative assays [19-20]. This is due to quick reduction of small volumes of the dye by the cells or perhaps high concentrations of resazurin salts having an inhibitory effect on cell growth and metabolism. For higher cell inoculums, the fluorescent signal easily reached saturation within a few minutes when a 5% (w/v) (5 μ L) dye concentration was used but a strong fluorescent signal after 4 hours incubation was obtained with 10% (10 μ L) resazurin. Therefore 10% resazurin was selected as an ideal dye concentration for all of the assays.

Nevertheless, the dye was linearly reduced proportionally to the incubation period (**Supplementary Figure 3**). However, for high cell densities such as 8×10^7 /mL and 4×10^7 /mL, the fluorescence signal reached saturation after 1 hour and 2 hrs incubation, respectively. However, after 4 hrs incubation, a very strong signal from 2×10^7 cells/mL gave the best maximum fluorescence to background signal ratio of 9:1. The reported signal to background ratio (S/B) is higher than the 3:1 obtained from *T. b. gambiense* but lower than that from *T. b. rhodesiense* (15:1) in similar assays [20]. These differences could be attributed to variations in dehydrogenase activity responsible for metabolizing resazurin or reduced uptake

of the dye substrate among the parasites. Differences in the fluorescence analysers, concentrations of the dye used, as well as the composition of media used to culture these parasites could potentially also account for some of the variations observed.

Since compounds library collections were diluted in DMSO, which is known to be toxic to cells at various concentrations, it was necessary to determine its effects on the viability of the *C. fasciculata* by exposing the parasites to various DMSO concentrations (**Supplementary Figure 4**). The *C. fasciculata* parasites were able to tolerate maximum DMSO concentrations of up to 0.5% with no significant decrease in fluorescent signal. This DMSO sensitivity is slightly higher than the 0.42% reported for bloodstream form *T. b. brucei* strain 427 by Sykes and Avery [18], but lower than the 1% reported for bloodstream forms of *T. brucei* strain 427 and *T. congolense* STIB910 [21]. One possible factor that may have resulted in such different observations of DMSO sensitivities might be the media used in each of the protocols. Different culture media can have different constituents which may positively or negatively react with the DMSO effecting the viability and consequently the doubling times of the parasites. The use of water to dilute compounds have been observed to possess significant effects on the cell viability and EC₅₀ value of the compounds possibly due to osmotic effect of water on cells and changes in the buffering capacity of the medium [19].

After optimizations, the assay performance and its capabilities to discriminate the activities of different compounds was evaluated by calculating the Z' factor [22]. Statistically, the assay performed well with an average Z' factor of 0.7 (a maximum plating cell density of 5 x 10⁴ cells/mL, 48 hrs incubation, 10% v/v resazurin and maximum of 0.5% DMSO). The distribution of Z' factor (a Z' factor between 1-0.5 is an acceptable for a robust assay) in a total of 100 randomly selected plates is shown (**Figure 1**). This showed that the assay was able to discriminate compounds with different levels of inhibition during the screening process.

Screening the chemical boxes for anti-crithidial compounds

Utilizing conditions established during optimization, the resazurin-based *C. fasciculata* assay was used to screen for anti-crithidial compounds from the open access MMV pathogen box and GSK Tres Cantos chemical boxes.

Using an inhibition cut-off of $\geq 80\%$, the primary screening of the MMV pathogen box led to the identification of 91 (23%) compounds with inhibitory activities at 100 μM against *C. fasciculata*. The dose-response experiments of the 91 compounds revealed 72 (79%) were true active compounds, representing an overall hit rate of 18% (**Figure 2**). The profiles and *in vitro* anti-crithidial activities of all compounds in the MMV pathogen box are shown (**Supplementary Table 1**). Ten compounds were picked based upon their potency and

selectivity from these confirmed true active compounds (**Table 1**). The screening revealed compounds (**1** and **6**) with a common 2-(pyridin-2-yl) pyrimidin-4-amine chemical scaffold and also compound **9** containing a pyrazol (3, 4) pyrimidin-4-amine. Derivatives of the pyrimidin-4-amine scaffold have been previously studied for their inhibitory activities against various protein kinase and cytochrome 51(CYP51) enzymes [15, 23]. The potency of compound **1**, a 2-pyridyl-4-aminopyrimidine derivative, is proposed to be due to it targeting methionine aminopeptidases in *Plasmodium*, and activity against all the three pathogenic kinetoplastids is also reported [14]. Of note, compounds **3**, **4** and **5** all have ~10 nM EC₅₀ values against *Crithidia*. Compound **5** bearing a diaminoquinazoline moiety known to target the dihydrofolate reductases, was also found to possess sub-micromolar inhibitory activity against asexual stage of *P. falciparum* parasites [14].

Using our predefined activity criteria (inhibition cut-off of $\geq 80\%$), the primary screening of a *T. brucei* GSK box identified a total of 66 (35%) compounds with inhibitory activities against *C. fasciculata* of which 42 (64%) were confirmed true active after retesting, representing an overall hit rate of 22% (**Figure 2**).

The primary screening of *T. cruzi* and *Leishmania* boxes revealed 101 (46%) and 122 (67%) compounds with inhibitory activities against *C. fasciculata*, of which 68 (67%) and 89 (73%) were confirmed true active after retesting, representing overall hit rates of 31% and 49%, respectively (**Figure 2**). The enriched hits rate observed after querying the GSK boxes may suggest the commonality of the targets shared between *C. fasciculata* and the *T. brucei*, *T. cruzi*, and *Leishmania* species. The higher hit rate observed from the *Leishmania* box is not surprising given the greater likelihood of conserved targets between *Leishmania* and *Crithidia* since they are phylogenetically closer to each other. The profiles and *in vitro* anti-crithidial activities of all compounds in the GSK *T. brucei*, *T. cruzi* and *Leishmania* boxes are shown in **Supplementary tables 2, 3 and 4**, respectively. The profiles of the ten most potent molecules from the confirmed active compounds in each of the GSK *T. brucei*, *T. cruzi* and *Leishmania* boxes are shown in **Tables 2, 3 and 4**, respectively.

The *T. brucei* GSK box revealed compound **14** contains exactly the same 2-(pyridin-2-yl) pyrimidin-4-amine scaffold as those highlighted above from the MMV box. Three compounds (**11**, **15** and **20**) contained a common 5-nitrofuran-2-yl scaffold, while the other five had distinct structures (**Table 2**). The nitro-substituted aryl group derivatives (**11**, **13**, **15** and **20**) are potential substrates for type I nitroreductase enzymes, responsible in various parasites for metabolising compounds into toxic nitrile products [24]. We observed Nifurtimox possesses a nanomolar potency (pIC₅₀: 7.8 \pm 0.003) against *C. fasciculata* which, as it undergoes the same

mode of action, suggests the functionality of type I nitroreductases in these parasites. However, as there are several nitro-heterocycles that have been shown to have a different mode of action [25], and with renewed interest in treating kinetoplastid diseases with nitro-drugs, such as Nifurtimox and Benznidazole [26], there is a call for further studies on the mode of action of the potent nitro-aromatic chemicals identified in these compound libraries. The 5-nitrofuran-2-yl derivatives are also known to inhibit *Mycobacterium tuberculosis* H37RV [27].

As there are no mammalian nitroreductase homologues, the 5-nitrofuran-2-yl derivatives are potentially useful in anti-parasitic therapy; however, it is well known that most nitro-aromatics are not well tolerated by the patients that take them and often they do not complete the therapeutic regime [5, 6].

Querying the *T. cruzi* box hits (**Table 3**) shows two more nitro-heterocyclic analogues (**21** and **22**). The relatively simple compound **29**, with a pIC₅₀ above 6, harbours a 1, 2, 3-thiadiazole-5-carboxamide moiety, which has been reported to have antifungal activity [28]. Of particular interest is compound **23** with a quinolin-8-ol moiety. The potency of compounds harbouring the quinolin-8-ol moieties against *P. falciparum*, *C. parvum*, and fungal species has been previously reported [29, 30]. Quinoline derivatives mefloquine, chloroquine and tafenoquine exhibit antimalarial activities as heme polymerase inhibitors, while sitamaquine has been reported for its anti-leishmanial activity.

The *Leishmania* box revealed three nanomolar hits (**31**, **32** and **40**) (**Table 4**) with the same 2-(pyridin-2-yl) pyrimidin-4-amine and the highly structurally related 2-(imidazolyl) pyrimidin-4-amine and (pyridin-2-yl) triazine-2-amine scaffolds, respectively. The heterocyclic pyridines and other pyridine fused ring systems are widely reported to associate with several biological activities [31].

Drugs derived from the pyrimidin-4-amine chemical class such as posaconazole are reported to clear *T. cruzi* in mouse models by inhibiting sterol 14 α -demethylase and consequently blocking sterol biosynthesis and therefore membrane formation [32-33]. Another well-known pyrimidine CYP51 inhibitor is a plant fungicide fenarimol reported to be effective against *T. cruzi* [34] as well as *Leishmania* [35]. Other studies have reported the inhibition of *T. cruzi* growth by 4-trifluoromethyl pyrimidine derivatives and a significant improvement in potency when the 5-pyrimidinyl group is replaced with 3-pyridinyl and the ring 1-*ortho*-chlorophenyl is replaced with a 4-trifluoromethylphenyl moiety [34, 35, 36]. Nonetheless, series of 2, 4-diaminopyrimidines analogues have been previously investigated and found to have *in vivo* efficacy against *Trypanosoma brucei* in an acute mouse model [37].

Collectively, the data presented here and reported elsewhere in the literature suggests that 2-(pyridin-2-yl) pyrimidin-4-amine (or a structurally similar scaffold) can form the basis of a pan-anti-kinetoplastid compound series targeting the same process in different kinetoplastids. In conclusion, we have developed a *C. fasciculata* viability assay that overcomes the limitations of safety and cost issues associated with drug discovery research in pathogenic kinetoplastids. The commonality of biological and cellular process between *C. fasciculata* and related pathogenic kinetoplastids shows the usefulness of this study to identify attractive chemical scaffolds within the GSK Tres Cantos and MMV boxes, providing valuable information for future efforts in anti-pathogenic kinetoplastid drug development.

Acknowledgements

We thank the MMV and GSK for the supply of the chemical boxes. We thank Peter Cockram for careful reading of the manuscript. This work was supported through the Global Health Implementation program at the University of St Andrews by the Gloag Foundation and the Western Union Foundation.

ACCEPTED MANUSCRIPT

References

1. Stuart K, Brun R, Croft S, Fairlamb A, Gürtler RE, McKerrow J, Reed S and Tarleton R (2008). Kinetoplastids: Related protozoan pathogens, different diseases. *J. Clin. Invest.* 118: 1301–10.
2. Kennedy PGE (2013). Clinical features, diagnosis and treatment of human African trypanosomiasis (sleeping sickness). *Lancet Neurology* 12: 186-194.
3. de Castro AM, Luquetti AO, Rassi A, Chiari E and Galvao LM (2006). Detection of parasitemia profiles by blood culture after treatment of human chronic *Trypanosoma cruzi* infection. *Parasitol. Res.* 99: 379–383.
4. Moraes CB, Giardini MA, Kim H, Franco CH, Araujo-Junior AM, Schenkman S, Chatelain E and Freitas-Junior LH. (2014). Nitroheterocyclic Compounds Are More Efficacious Than CYP51 Inhibitors against *Trypanosoma cruzi*: Implications for Chagas Disease Drug Discovery and Development. *Sci. Rep.* 4: 4703.
5. Field MC, Horn D, Fairlamb AH, Ferguson MA, Gray DW, Read KD, De Rycker M, Torrie LS, Wyatt PG, Wyllie S and Gilbert IH(2017). Anti-trypanosomatid drug discovery: an ongoing challenge and a continuing need. *Nat Rev Microbiol.* 15: 217-231.
6. Dias CPD, Coura JR and Yasuda MAS (2014). The Present Situation, Challenges and Perspectives Regarding the Production and Utilization of Effective Drugs against Human Chagas Disease. *Rev. Soc. Bras. Med. Trop.* 47: 123–125.
7. Podesta D, Stoppani A, Villamil SF (2003) Inactivation of *Trypanosoma cruzi* and *Crithidia fasciculata* topoisomerase I by Fenton systems. *Redox Rep* 8: 357–363.
8. Sinha KM, Hines JC, Downey N, Ray DS (2004) Mitochondrial DNA ligase in *Crithidia fasciculata*. *Proc. Natl. Acad. Sci. USA* 30: 4361–4366.
9. Liu B, Liu Y, Motyka SA, Agbo EE, Englund PT (2005) Fellowship of the rings: the replication of kinetoplast DNA. *Trends Parasitol.* 21: 363–369.
10. Sahin A, Lemercier G, Tetaud E, Espiau B, Myler P, Stuart K, et al (2004) Trypanosomatid flagellum biogenesis: ARL-3A is involved in several species. *Exp. Parasitol.* 108: 126–133.
11. Gadelha C, LeBowitz JH, Manning J, Seebeck T, Gull K (2004) Relationships between the major kinetoplastid paraflagellar rod proteins: a consolidating nomenclature. *Mol Biochem Parasitol* 136: 113–115.
12. Comini M, Menge U, Wissing J, Flohe L. (2005) Trypanothione synthesis in crithidia revisited. *J Biol Chem* 280: 6850–6860.

13. Škodová-Sveráková, I., Verner, Z., Skalický, T., Votýpka, J., Horváth, A. and Lukeš, J. (2015), Lineage-specific activities of a multipotent mitochondrion of trypanosomatid flagellates. *Molecular Microbiology*, 96: 55–67.
14. Duffy S, Sykes ML, Jones AJ, Shelper TB, Simpson M, Lang R, Poulsen SA, Sleeb BE and Avery VM (2017). Screening the MMV Pathogen Box across multiple pathogens reclassifies starting points for open source drug discovery. *Antimicrob. Agents Chemother.* AAC.00379-17.
15. Peña I, Manzano PM, Cantizani J, Kessler A, Alonso-Padilla J, Bardera AI, Alvarez E, Colmenarejo G, Cotillo I, Roquero I, de Dios-Anton F, Barroso V, Rodriguez A, Gray DW, Navarro M, Kumar V, Sherstnev A, Drewry DH, Brown JR, Fiandor JM, Martin JJ (2015). New compound sets identified from high throughput phenotypic screening against three kinetoplastid parasites: an open resource. *Sci. Reports* 5: 8771.
16. Calderón-Arguedas OCM, Avendaño A, Carvajal MJ (2006). Multiplicative kinetics of *Crithidia fasciculata* (Kinetoplastida: Trypanosomatidae) clones in an *in vitro* culture system. *Parasitol Latinoam* 61: 32–36.
17. Scolaro EJ, Ames RP and Brittingham A (2005). Growth-phase dependent substrate adhesion in *Crithidia fasciculata*. *J Eukaryot Microbiol.* 52: 17-22.
18. Popp M and Lattorff HM (2011). Quantitative *in vitro* cultivation technique to determine cell number and growth rates in strains of *Crithidia bombi* (Trypanosomatidae), a parasite of bumblebees. *J Eukaryot Microbiol.* 58: 7-10.
19. Sykes ML and Avery VM (2009). Development of an Alamar Blue™ viability assay in 384-well format for high throughput whole cell screening of *Trypanosoma brucei brucei* bloodstream form strain 427. *Am. J. Trop. Med. Hyg.* 81: 665–674.
20. Ráz B, Iten M, Grether-Bühler Y, Kaminsky R and Brun R (1997). The Alamar Blue assay to determine drug sensitivity of African trypanosomes (*T. b. rhodesiense* and *T. b. gambiense*) *in vitro*. *Acta Trop.* 68: 139–147.
21. Merschjohann K and Steverding D. (2006) *In vitro* growth inhibition of bloodstream forms of *Trypanosoma brucei* and *Trypanosoma congolense* by iron chelators. *Kinetoplastid Biol Dis.* 5: 3.
22. Zhang JH, Chung TD and Oldenburg KR (1999). A simple statistical parameter for use in evaluation and validation of high throughput screening assays. *J Biomol Screen* 4: 67–73.
23. Gunatilleke SS, Calvet CM, Johnston JB, Chen CK, Erenburg G, Gut J, Engel JC, Ang KK, Mulvaney J, Chen S, Arkin MR, McKerrow JH, Podust LM (2012). Diverse

- inhibitor chemotypes targeting *Trypanosoma cruzi* CYP51. *PLoS Negl. Trop. Dis.* 6: e1736.
24. Hall BS, Bot C and Wilkinson SR (2011). Nifurtimox activation by trypanosomal type I nitroreductases generates cytotoxic nitrile metabolites. *J. Biol. Chem.* 286: 13088–13095.
25. Zhou L, Stewart G, Rideau E, Westwood NJ, Smith TK (2013). A class of 5-nitro-2-furancarboxylamides with potent trypanocidal activity against *Trypanosoma brucei* *in vitro*. *J Med Chem.* 56: 796-806.
26. Patterson S and Wyllie S (2014). Nitro drugs for the treatment of trypanosomatid diseases: past, present, and future prospects. *Trends Parasitol.* 30: 289–298.
27. Doreswamy and Vastrad CM (2013). Predictive comparative QSAR analysis of as 5-Nitrofuran-2-YL derivatives in *Mycobacterium tuberculosis* H37RV. *Health Informatics- An International Journal (HIJ)* Vol.2, No.4. DOI: 10.5121/hij.2013.2404
28. Xu WM, Li SZ, He M, Yang S, Li XY and Li P (2013). Synthesis and bioactivities of novel thioether/sulfone derivatives containing 1, 2, 3-thiadiazole and 1,3,4 oxadiazole/thiadiazole moiety. *Bioorg Med Chem Lett.* 23: 5821-4.
29. Spangenberg T, Burrows JN, Kowalczyk P, McDonald S, Wells TN, Willis P. (2013) The open access malaria box: a drug discovery catalyst for neglected diseases. *PLoS One.* 8: e62906-10.1371/journal.pone.0062906.
30. Musiol R, Jampilek J, Buchta V, Niedbala H, Podeszwa B, Palka A, Majerz-Maniecka K, Oleksyn B, Polanski J (2006). Antifungal properties of new series of quinoline derivatives. *Bioorg. Med. Chem.* 14: 3592–3598.
31. Asif, M (2016) Biological Potential and Chemical Properties of Pyridine and Piperidine Fused Pyridazine Compounds: Pyridopyridazine a Versatile Nucleus *Asian Journal of Chemistry and Pharmaceutical Sciences, Vol 1(1), 2016, 29-35*
32. Doyle PS, Chen CK, Johnston JB, Hopkins SD, Leung SS, Jacobson MP, Engel JC, McKerrow JH, Podust LM (2010). A nonazole CYP51 inhibitor cures Chagas disease in a mouse model of acute infection. *Antimicrob. Agents Chemother.* 54: 2480–2488.
33. Lepesheva GI, Villalta F and Waterman MR (2011). Targeting *Trypanosoma cruzi* sterol 14 α -demethylase (CYP51). *Adv. Parasitol.* 75, 65–87.
34. Choi JY, Podust LM and Roush WR (2014). Drug Strategies Targeting CYP51 in Neglected Tropical Diseases. *Chem. Rev.* 114: 11242–11271.
35. Hargrove TY, Wawrzak Z, Alexander PW, Chaplin JH, Keenan M, Charman SA, Perez CJ, Waterman MR, Chatelain E, Lepesheva GI (2013). Complexes of *Trypanosoma*

- cruzi* sterol 14 α -demethylase (CYP51) with two pyridine-based drug candidates for Chagas disease: structural basis for pathogen selectivity. *J. Biol. Chem.* 288: 31602.
36. Zanatta N, Amaral SS, Dos Santos JM, de Mello DL, Fernandes Lda S, Bonacorso HG, Martins MA, Andricopulo AD, Borchhardt DM (2008). Convergent synthesis and cruzain inhibitory activity of novel 2-(N'-benzylidenehydrazino)-4-trifluoromethylpyrimidines. *Bioorg Med Chem.* 16: 10236-43.
37. Perales JB, Freeman J, Bacchi CJ, Bowling T, Don R, Gaukel E, Mercer L, Moore JA 3rd, Nare B, Nguyen TM, Noe RA, Randolph R, Rewerts C, Wring SA, Yarlett N, Jacobs RT (2011). SAR of 2-amino and 2,4-diamino pyrimidines with *in vivo* efficacy against *Trypanosoma brucei*. *Bioorg Med Chem Lett.* 21: 2816-9.

Figure 1. Distribution of Z' in a total of 100 plates randomly selected from the MMV (plates 1-25) and; GSK *T. brucei* (plates 26-50), *T. cruzi* (plates 51-75) and *Leishmania* (plates 76-100) boxes.

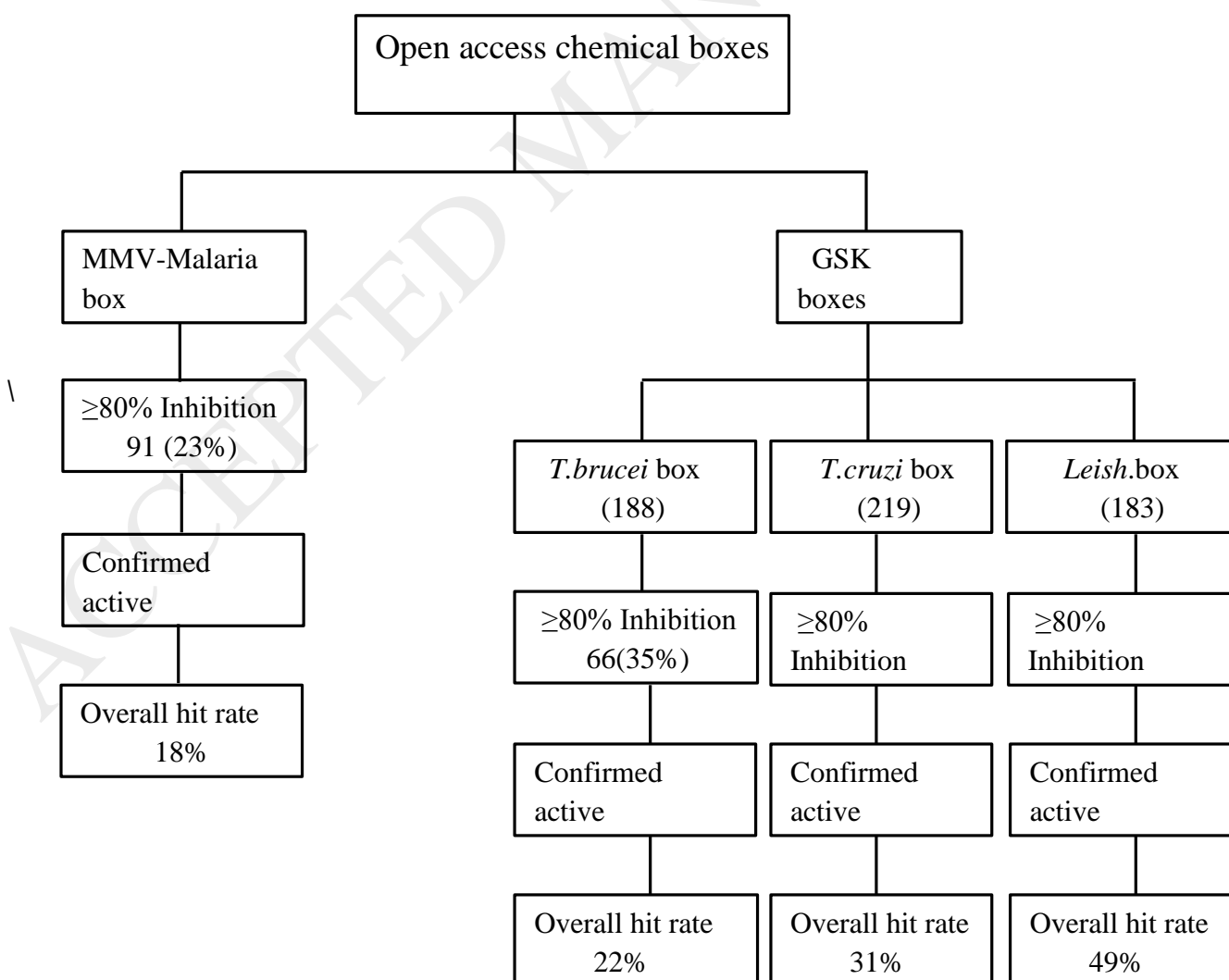
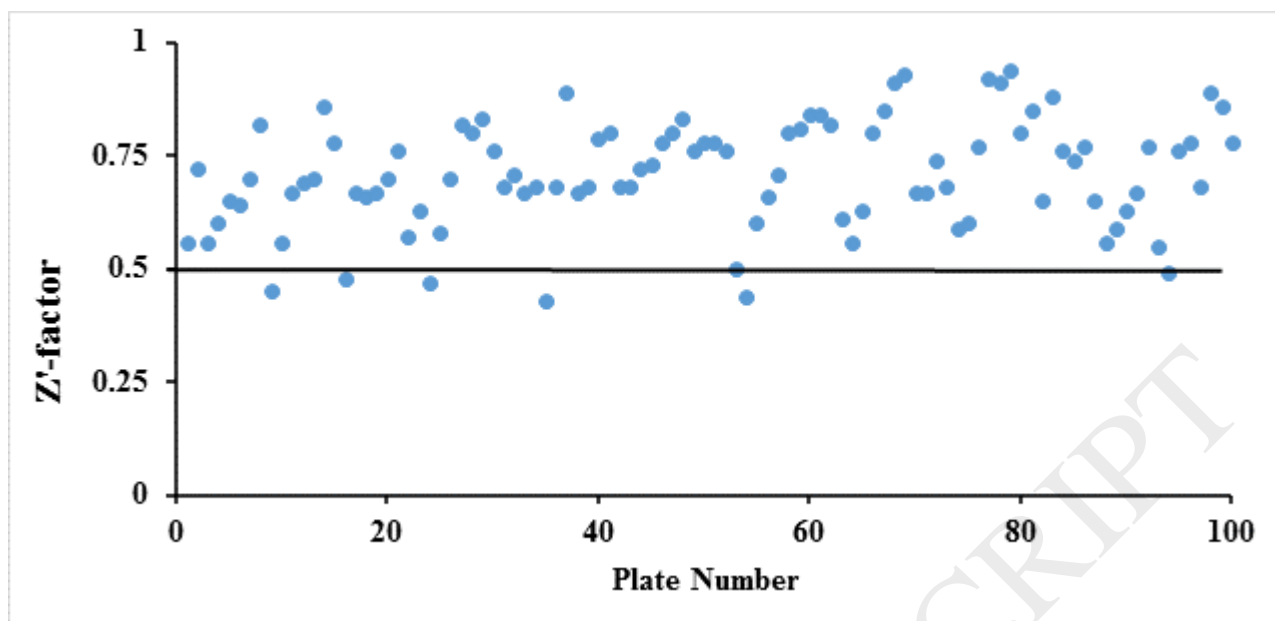
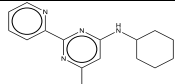
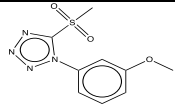
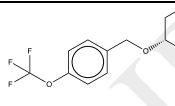
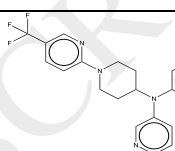
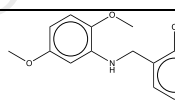
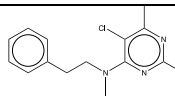
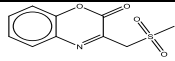
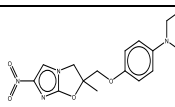
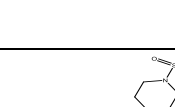
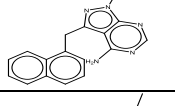


Figure 2. The flow diagram used to identify and progress hits of the open access pathogen boxes including key criteria considered in the decision-making process. In this case, all the compounds that had inhibition of $\geq 80\%$ were progressed to dose-response experiments to determine their EC_{50} values. True active compounds are those that had a $\geq 80\%$ inhibition and showed an EC_{50} in dose-response experiments.

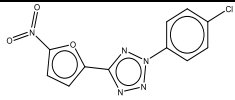
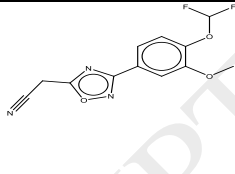
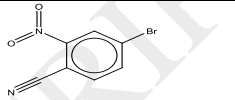
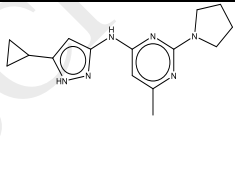
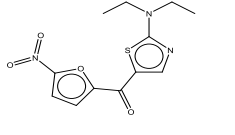
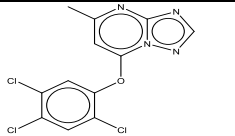
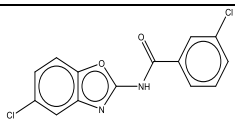
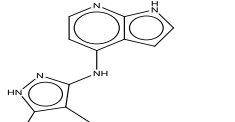
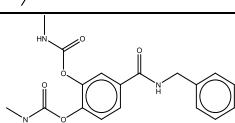
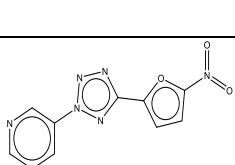
ACCEPTED MANUSCRIPT

Table 1. Profiles of the top ten hits identified from screening of the MMV pathogen box.

Compound ID	pEC50	cLogP	Compound name	Mol wt	Structure of the compound
1 MMV0 21013	7.4 ± 0.004	3.55	N-cyclohexyl-6-cyclopropyl-2-(pyridin-2-yl)pyrimidin-4-amine	294.40	
2 MMV2 72144	7.7 ± 0.03	-0.27	1-(3-methoxyphenyl)-5-(methylsulfonyl)-1H-tetrazole	254.27	
3 MMV6 88755	8.0 ± 0.001	2.81	(S)-2-nitro-6-((4-(trifluoromethoxy)benzyl)oxy)-6,7-dihydro-5H-imidazo[2,1-β][1,3]oxazine	359.26	
4 MMV6 89243	8.0 ± 0.003	4.26	N-(4-(trifluoromethyl)phenyl)-N-(1-(5-(trifluoromethyl)pyridin-2-yl)piperidin-4-yl)pyridin-3-amine	466.42	
5 MMV6 75968	8.0 ± 0.005	2.31	5-chloro-6-(((2,5-dimethoxyphenyl)amino)methyl)quinazoline-2,4-diamine	359.81	
6 MMV6 58988	6.1 ± 0.01	3.93	5-chloro-N,6-dimethyl-N-phenethyl-2-(pyridin-2-yl)pyrimidin-4-amine	338.84	
7 MMV5 53002	6.3 ± 0.1	-0.31	3-((methylsulfonyl)methyl)-2H-benzo[β][1,4]oxazin-2-one	239.25	
8 MMV6 88262	7.0 ± 0.04	5.04	2-methyl-6-nitro-2-(((4-(4-(4-(trifluoromethoxy)phenoxy)piperidin-1-yl)phenoxy)methyl)-2,3-dihydroimidazo[2,1-b]oxazole	534.48	
9 MMV6 88470	6.1 ± 0.02	3.12	1-(2-(1-(methylsulfonyl)piperidin-4-yl)ethyl)-3-(naphthalen-1-ylmethyl)-1H-pyrazolo[3,4-d]pyrimidin-4-amine	464.58	
10 MMV6 76445	6.1 ± 0.01	2.71	2-(((1-propyl-1H-benzo[d]imidazol-2-yl)methyl)amino)phenol	281.35	

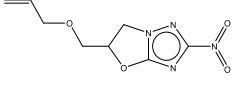
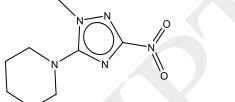
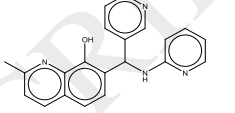
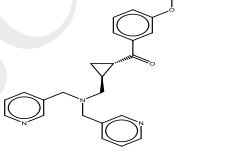
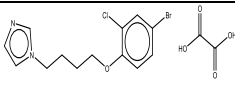
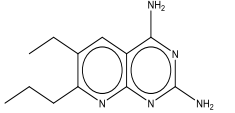
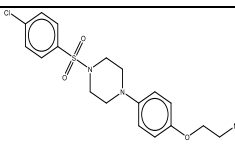
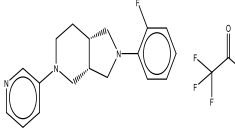
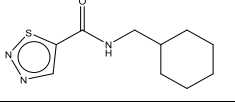
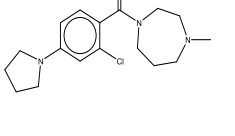
The cytotoxicity data and other relevant information of these compounds are found at (<http://www.pathogenbox.org/about-pathogen-box/supportinginformation>). pIC₅₀ values are means of two independent assays, which varied < ±50%.

Table 2. Profile of ten top hit compounds identified in the GSK *T. brucei* box

Compound ID	pEC50	Cyto-toxicity (pIC50)	cLogP	Compound name	Mol wt	Structure of the compound
11 TCMDC-143074	5.5 ± 0.3	<4.0	3.422	2-(4-chlorophenyl)-5-(5-nitrofur-2-yl)-2H-tetrazole	291.65	
12 TCMDC-143457	5.4 ± 0.01	<4.0	1.21	2-(3-(4-(difluoromethoxy)-3-methoxyphenyl)-1,2,4-oxadiazol-5-yl)acetonitrile	281.22	
13 TCMDC-143609	5.4 ± 0.2	4.7	1.881	4-bromo-2-nitrobenzonitrile	227.02	
14 TCMDC-143363	5.3 ± 0.03	4.5	2.772	N-(5-cyclopropyl-1H-pyrazol-3-yl)-6-methyl-2-(pyrrolidin-1-yl)pyrimidin-4-amine	284.37	
15 TCMDC-143112	5.3 ± 0.1	4.8	2.654	(2-(diethylamino)thiazol-5-yl)(5-nitrofur-2-yl)methanone	295.32	
16 TCMDC-143316	5.1 ± 0.5	4.5	3.74	5-methyl-7-(2,4,5-trichlorophenoxy)-[1,2,4]triazolo[1,5-α]pyrimidine	329.58	
17 TCMDC-143172	5.0 ± 1.0	<4.0	4.29	3-chloro-N-(5-chlorobenzo[δ]oxazol-2-yl)benzamide	307.13	
18 TCMDC-143460	5.0 ± 0.7	<4.0	2.383	N-(4,5-dimethyl-1H-pyrazol-3-yl)-1H-pyrrolo[2,3-b]pyridin-4-amine	227.27	
19 TCMDC-143079	5.0 ± 0.04	<4.0	1.358	4-(benzylcarbamoyl)-1,2-phenylene bis(methylcarbamate)	357.36	
20 TCMDC-143073	5.0 ± 0.3	<4.0	1.212	3-(5-(5-nitrofur-2-yl)-2H-tetrazol-2-yl)pyridine	258.20	

Data on cytotoxicity and other information about these compounds is found on (<https://www.ebi.ac.uk/chemblntd>). pIC₅₀ values are means of two independent assays, which varied < ±50%.

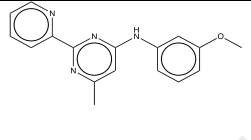
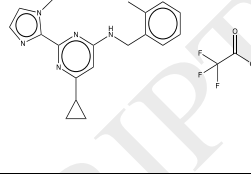
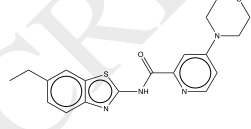
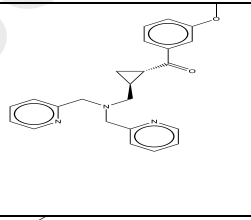
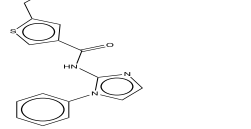
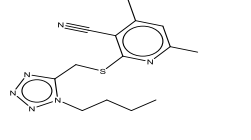
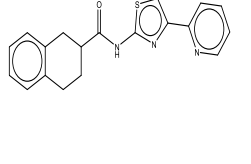
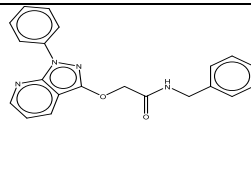
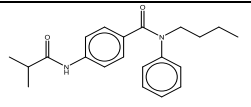
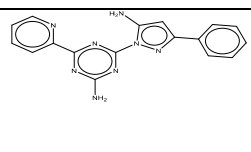
Table 3. Profile of ten top hit compounds identified in the GSK *T. cruzi* box

Compound ID	pEC50	Cyto-toxicity (pIC50)	cLogP	Compound name	Mwt	Structure of the compound
21 TCMDC-143149	5.9 ± 0.05	<4.0	-0.242	5-((allyloxy)methyl)-2-nitro-5,6-dihydrooxazolo[3,2-β][1,2,4]triazole	226.19	
22 TCMDC-143088	5.6 ± 0.1	<4.0	0.432	1-(1-methyl-3-nitro-1H-1,2,4-triazol-5-yl)piperidine	211.22	
23 TCMDC-143308	5.7 ± 0.01	4.7	2.799	2-methyl-7-(pyridin-2-ylamino)(pyridin-3-yl)methylquinolin-8ol	342.39	
24 TCMDC-143593	5.8 ± 0.03	<4.0	3.005	((1S,2S)-2-((bis(pyridin-3-yl-methyl)amino)methyl)cyclopropyl)(3-methoxyphenyl)methanone	387.47	
25 TCMDC-143590	5.7 ± 0.07	4.3	3.947	1-(4-(4-bromo-2-chlorophenoxy)butyl)-1H-imidazole oxalate	419.66	
26 TCMDC-143606	5.6 ± 0.01	4.7	2.666	6-ethyl-7-propylpyrido [2,3-δ] pyrimidine -2,4-diamine	231.30	
27 TCMDC-143622	6.5 ± 0.02	4.3	4.109	2-(4-(4-((4-chlorophenyl)sulfonyl)piperazin-1-yl)phenoxy)-N,N-dimethylethan-1-amine	423.96	
28 TCMDC-143422	6.2 ± 0.05	<4.0	3.173	(3aS,7aS)-2-(2-fluorophenyl)-5-(pyridin-3-yl)octahydro-1H-pyrrolo[3,4-c]pyridine .TFA	411.39	
29 TCMDC-143612	6.3 ± 0.003	4.4	1.913	N(cyclohexylmethyl) -1,2,3-thiadiazole-5-carboxamide	225.31	
30 TCMDC-143127	5.7 ± 0.01	<4.0	2.525	(2-chloro-4-(pyrrolidin-1-yl)phenyl)(4-methyl-1,4-diazepan-1-yl)methanone	321.85	

Data on cytotoxicity and other information about these compounds is found on (<https://www.ebi.ac.uk/chemblntd>). pIC_{50} values are means of two independent assays, which varied $< \pm 50\%$.

ACCEPTED MANUSCRIPT

Table 4. Profile of ten top hit compounds identified in the GSK Leish box

Compound ID		pEC50	Cyto-toxicity (pIC50)	cLogP	Compound name	Mol wt	Compound structure
31	TCMDC-143621	6.9 ± 0.01	4.3	3.7	<i>N</i> -(3-methoxyphenyl)-6-methyl-2-(pyridin-2-yl)pyrimidin-4-amine	292.34	
32	TCMDC-143487	6.8 ± 0.003	4.8	3.597	6-cyclopropyl-2-(1-methyl-1 <i>H</i> -imidazol-2-yl)- <i>N</i> -(2-methylbenzyl)pyrimidin-4-amine	433.44	
33	TCMDC-143239	6.0 ± 0.2	<4.0	3.648	<i>N</i> -(6 ethylbenzo[<i>d</i>]thiazol-2-yl)-4 morpholinopicolinamide	368.46	
34	TCMDC-143586	6.0 ± 0.02	4.0	3.005	((1 <i>S</i> ,2 <i>S</i>)-2-((bis(pyridin-2-ylmethyl)amino)methyl)cyclopropyl)(3-methoxyphenyl)methanone	387.47	
35	TCMDC-143375	5.9 ± 0.1	<4.0	4.188	5-ethyl- <i>N</i> -(1-phenyl-1 <i>H</i> -imidazol-2-yl)thiophene-3-carboxamide	297.38	
36	TCMDC-143315	5.6 ± 0.06	<4.0	3.07	2-(((1-butyl-1 <i>H</i> -tetrazol-5-yl)methyl)thio)-4,6-dimethylnicotinonitril	302.40	
37	TCMDC-143113	5.5 ± 0.2	4.4	3.856	<i>N</i> -(4-(pyridin-2-yl)thiazol-2-yl)-1,2,3,4-tetrahydronaphthalene-2-carboxamide	335.43	
38	TCMDC-143358	5.4 ± 0.01	<4.0	3.349	<i>N</i> -benzyl-2-((1-phenyl-1 <i>H</i> -pyrazolo[3,4- <i>b</i>]pyridin-3-yl)oxy)acetamide	358.39	
39	TCMDC-143252	5.5 ± 0.5	<4.0	4.289	<i>N</i> -butyl-4-isobutyramido- <i>N</i> -phenylbenzamide	338.44	
40	TCMDC-143218	5.5 ± 0.3	5.0	1.55	4-(5-amino-3-phenyl-1 <i>H</i> -pyrazol-1-yl)-6-(pyridin-2-yl)-1,3,5-triazin-2-amine.TFA	1242.5	

Data on cytotoxicity and other information about these compounds is found on (<https://www.ebi.ac.uk/chemblntd>). pIC_{50} values are means of two independent assays, which varied $< \pm 50\%$.

ACCEPTED MANUSCRIPT